InGaAlAsPN: A MATERIALS SYSTEM FOR SILICON BASED OPTOELECTRONICS AND HETEROSTRUCTURE DEVICE TECHNOLOGIES

T. P. E. Broekaert*, S. Tang, R. M. Wallace, E. A. Beam III, W. M. Duncan, Y.-C. Kao, H.-Y. Liu

System Components Laboratory

and

Materials Science Laboratory

IS&S Corporate R&D, Texas Instruments, Dallas, TX 75265

ABSTRACT

A new material system is proposed for silicon based optoelectronic and heterostructure devices: the silicon lattice matched compositions of the (In,Ga,Al)-(As,P)N III-V compounds. In this nitride alloy material system the bandgap is expected to be direct at the silicon lattice-matched compositions with a bandgap range most likely to be in the infrared to visible. At lattice constants ranging between those of silicon carbide and silicon, a wider bandgap range is expected to be available and the high quality material obtained through lattice matching could enable applications such as monolithic color displays, high efficiency multi-junction solar cells, optoelectronic integrated circuits for fiber communications, and transfer of existing III-V technology to silicon.

1. Introduction

Recently, the growth of the $GaAs_xN_{1-x}$[1,2,3,4,5] compound semiconductors has been gaining interest. This increased interest in nitride based semiconductors is primarily related to the potential for short wavelength (blue and violet) emitting devices[6,7] and the capability of the arsenide nitride compound semiconductors of being lattice-matched to silicon[3]. This combination of direct bandgap materials and the potential for high quality lattice-matched crystalline materials on a silicon substrate is heretofore unrealized and is ideal for silicon-based optoelectronics[8]. However, the applications for this material system are potentially much broader, depending on the range of bandgaps that will be available. The ternaries of interest that lattice match to silicon are, assuming that Vegard's law holds for the III-V N alloys, $AlAs_{0.82}N_{0.18}$, $GaAs_{0.81}N_{0.19}$, $InAs_{0.41}N_{0.59}$, $InP_{0.5}N_{0.5}$. Thus, the silicon based ternaries all require large amounts of nitrogen to be incorporated. The binaries GaP and AlP nearly lattice match to silicon but are of limited interest for electro-optic devices owing to their indirect bandgap. However, strained pseudomorphic layers of GaP_xN_{1-x} and AlP_xN_{1-x} may be of use in devices with nanometer scale layer thicknesses.

2. Challenges and opportunities

The challenge in growing the group III - V nitride alloy compounds is due to the large difference in the atomic radii of nitrogen and the other group V elements. Such material systems with large differences in atomic radii are known to have large miscibility gaps and cannot be grown by equilibrium techniques[9]. However, immiscible material systems can be grown by non-equilibrium techniques

such as MBE. Indeed, immiscible materials with large microscopic strain such as $GaP_{1-x}Sb_x$[10] and $(GaAs)_{1-x}Si_x$[11] have already been grown successfully. Two questions need to be answered to determine the potential of these heterojunction materials : (1) Are any of the large-nitrogen-content alloys (meta-) stable? and (2) what bandgap range is possible?

Concerning question (1), the high microscopic strain in the III-V N alloys is expected to lead to ordering[12] which is known to stabilize the epitaxial layers[13] and to change the bandgap as compared to the bandgap of the random alloy[14]. For x=0.5 alloys, the chalcopyrite ordering typically results in an increased bandgap, while CuAu or CuPt type ordering typically lowers the bandgap as compared to that of the random alloy[14]. Epitaxial stabilization in ordered compounds is strongest for the stoichiometric compound[13], x=0.5, with decreasing stability towards the constituents. Thus, $InP_{0.5}N_{0.5}$ may form a stable ordered chalcopyrite compound, while decreasing epitaxial stability against decomposition is expected for $InAs_{0.41}N_{0.59}$, $GaAs_{0.81}N_{0.19}$ and $AlAs_{0.82}N_{0.18}$. As an example, in the case of $InAs_{0.41}N_{0.59}$ the ordering may result in $InAs_{0.41}N_{0.59}$ being an alloy of the chalcopyrite-like In_2AsN and the famatinite-like In_4AsN_3, or as an $In_5As_2N_3$ ordered compound, rather than a random alloy of InAs and InN. For quaternary alloys such as the AlGaAsN compounds on silicon an ordered group V sublattice would be expected, while the group III sublattice can be random owing to the similar radii of gallium and aluminum.

The second question is that of the bandgap range available in the III-V N compounds. Munich and Pierret first calculated the bandgaps for AlGaAsN compounds[15], in particular, for the silicon matched compounds they find a direct-bandgap range of about 1.7 eV to 3.0 eV. However, they did not take into account the extrinsic bowing as described by Van Vechten and Bergstresser[16]. On the other hand, Sakai[6] et al. by taking into account the extrinsic bowing predict a semimetallic nature (zero bandgap) over a wide range of the (InAlGa)(SbAsP)N compounds. The "negative" bandgaps predicted correspond to a structure that has zero bandgap between the main conduction and valence bands but that has negative E_0, i.e. an inverted band structure as in $Hg_xCd_{1-x}Te$[17]. However, the extrapolations used in Ref. 6 to calculate the bandgap at high alloy concentrations, i.e. $x \approx 0.5$, may be beyond the validity of the model used, as described in Ref. 16, since the perturbation potential caused by the alloying has become sufficiently large to affect the character of the valence and conduction bands. An ab initio calculation is needed to obtain a more reliable theoretical estimate. Recently Rubio and Cohen[18] calculated a finite bandgap of 0.7 eV for $GaAs_{0.75}N_{0.25}$ using the local density approximation (LDA) without, however, internal relaxation of the crystal structure. Neugebauer and Van de Walle[19] calculated the bandstructure for a (111) superlattice of $GaAs_{0.5}N_{0.5}$ with internal relaxation and found a zero bandgap metallic structure. Recent results obtained by Tang[20] et. al. at Texas Instruments using LDA with internal relaxation have shown that some of the ordered structures of $GaAs_{0.5}N_{0.5}$ and $GaAs_{0.75}N_{0.25}$ have a finite bandgap.

Preliminary experimental bandgap results at large nitrogen content are so far inconclusive[3]. The bandgap range available in the nitride alloy system is thus still open to debate. An estimate can be made for the random alloys using the recently obtained experimental values for the bowing coefficient in $GaAs_xN_{1-x}$[1,5] (18 eV) and GaP_xN_{1-x}[21] (14 eV). As pointed out in the previous section the bandgap values obtained at high alloy concentrations using this method may not be accurate. Figure

l shows the estimated bandgap versus lattice constant for the ternaries of the InGaAlAsPN material system, using a bowing coefficient of 14 eV for the phosphide nitrides and 18 eV for the arsenide nitrides. The solid lines represent the Γ-point bandgap while the dashed lines represent the X-point bandgap. Also shown in figure l is the estimated bandgap for the Famatinite ordered $GaAs_{0.75}N_{0.25}$. Although the bandgap range that would be available on silicon is still uncertain, the early indications are that the range will be in the infrared to red part of the spectrum, enabling such applications as 1.55 µm detectors and lasers, and devices such as FETs and HBTs using the low bandgap Al-GaAsN quaternaries. At lattice constants smaller than that of silicon, alloys covering the entire visible bandgap range might be feasible, enabling applications such as color displays and high efficiency multijunction solar cells.

As a result of the strong bowing in the III-V N alloys which shifts the bandgap towards the infrared, the applications requiring a red to blue wavelength bandgap range such as color displays and high efficiency multijunction solar cells may need to be grown on smaller lattice constant materials, e.g. Si_xC_{1-x} with x = 0.75 to x = 0.60 as most likely.
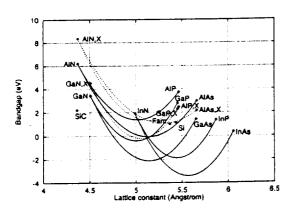

Figure 1. Bandgap vs. lattice constant in the In-GaAlAsPN material system. The solid lines represent empirical extrapolation from low nitrogen content alloys for the direct bandgap, while the dashed lines represent the X-point. The point labeled Fam. is the ab-initio theoretical prediction for the bandgap of Famatinite $GaAs_{0.75}N_{0.25}$.

bandgap range on silicon is possibly more limited, several heterostructure devices are possible using AlGaAsN quaternaries. For example a resonant tunneling diode could be made using AlAsN as the barrier material and GaAsN as the well and contact material. Similarly, FETs and HBTs can be made using the AlGaAsN quaternaries. In addition, the piezoelectric properties of III-V semiconductors in general and of the nitride alloys in specific would

Therefore, the growth of high quality lattice-matched materials covering a bandgap range as wide as the entire visible range on a single substrate may be achieved, making possible the monolithic integration of full color displays and detectors. As with other material systems quaternaries can be used for bandgap engineering and device optimization. An example of the versatility possible with a wide available bandgap range is shown in figure 2: by making use of the optical low pass nature of semi-conductors, a true multi-color pixel can be achieved by vertically stacking the red, green and blue pixel of a color display. The vertical stacking results in a pixel with a true color appearance irrespective of viewing angle and distance. Though the
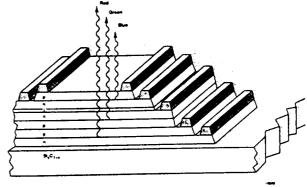

Figure 2. A true color pixel as an example of one of the new applications possible with the InGaAlAsPN material system.

allow the integration of surface acoustic wave devices on silicon.

Finally, it should be noted that due to the uncertainty of theoretical predictions of bandgaps that the actual bandgap range of the InGaAlAsPN compounds will not be accurately known until it is experimentally determined.

3. Experimental results

Several methods have been used in this study for the growth of $GaAs_{1-x}N_x$ alloys. The first method used in this study is MOMBE: a metalorganic source is used for the arsenic (TBA or TDMAAs) and a solid source is used for the group III elements; an ECR nitrogen source is used for the nitrogen supply. A number of varying nitrogen flow rates, ECR power and substrate temperature were used for the growth. The initial choice of substrates in this study is GaAs to avoid the antiphase domain boundary defects that would be associated with growth on silicon. All films had a rough surface with a hazy to orange peel look. At high substrate temperatures, 600 °C, the epitaxial material formed is a polycrystalline cubic GaN film. For one of the growths, at low substrate temperature, 500 °C, a polycrystalline film is formed which has been identified as having two major components: a $GaAs_{1-x}N_x$ compound with a nitrogen content of about 6.5% and a second compound Ga_3As_2N, i.e. with 33 % nitrogen. Figure 3 shows the thin film X-ray diffraction pattern for the polycrystalline film containing Ga_3As_2N [22]. Three of the intensity X-ray peaks are identified as (111), (220), and (400) reflections of $GaAs_{1-x}N_x$ with x = 6.54%. Two of the other peaks are identified as (111) and (224) reflections of $GaAs_{1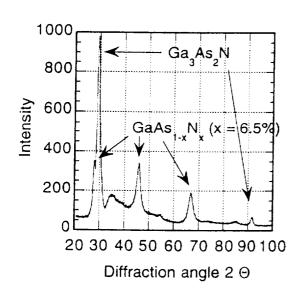-x}N_x$ with x = 33.75%. This last result of a nitrogen fraction of 33.75% is interesting since it indicates that high nitrogen fraction compounds can be formed. Moreover, the close to 2 to 1 ratio of As to N suggests that this material system may be likely to form ordered compounds at high nitrogen fractions.

The second method used to grow the $GaAs_{1-x}N_x$ alloys in this study is conventional MBE: solid sources are used for both group III and group V elements, except for the nitrogen which is again provided for by an ECR nitrogen source. At small nitrogen fractions up to 1.5% it is possible to obtain a single crystal epitaxial film and the bandgap of the material has a red shift with increasing nitrogen fraction with a bowing coefficient of about 18 eV as has been previously obtained in other studies[1,2]. Figure 4 shows the bandgap dependence of $GaAs_xN_{1-x}$ at small nitrogen fractions[23]. Also shown in the same figure is the empirical bandgap dependence assuming an 18 eV bowing coefficient.

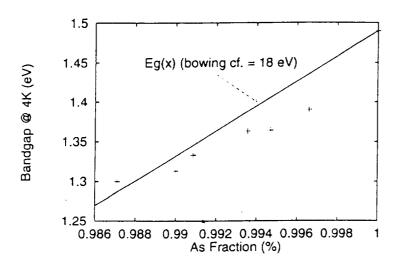Figure 3. Thin film X-ray diffraction of a polycrystalline sample grown by MOMBE.
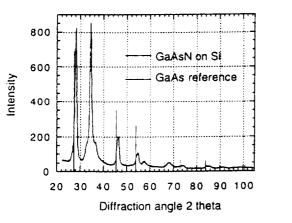
Figure 4. Bandgap of $GaAs_xN_{1-x}$ as a function of As fraction as measured by PL at 4 K.

For films with greater than 1.5% nitrogen no single crystal epitaxial film has been obtained to date. Again, a polycrystalline film is obtained for the higher nitrogen fraction films. Figure 5 shows the thin film diffraction pattern of such a polycrystalline film, one grown on silicon and the other on GaAs. The large peak at 34.5 degree is associated with (111) cubic GaN or $GaAs_xN_{1-x}$ with a small As fraction. Three peaks are identified as $GaAs_{1-x}N_x$: the peaks near 28, 46, and 54 degree are associated with (111), (220), and (311) crystal plane reflections. Assuming Vegard's law, and without correcting for strain deformation, the nitrogen composition associated with each peak is 25.5%, 2.8%, and 5.8% for the GaAs substrate based sample and 11.7%, 9.7%, and 9.7% for the silicon substrate based sample respectively. Due to the polycrystalline nature of the film it is not possible to determine the amount of strain deformation, and therefore also the true nitrogen content, in each of the differently oriented grains. From the silicon substrate based sample one can conlude that the nitrogen content is at least 10%.
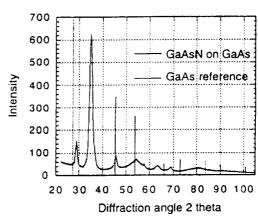

Figure 5. Thin film X-ray diffraction of GaAsN grown on silicon (shown on the left) and on GaAs (shown on the right) in comparison to a GaAs reference diffraction pattern.

Thus far we have not been successful at detecting any photoluminescence from the high nitrogen fraction compounds observed here, which leaves open the question of the electronic properties of the high nitrogen fraction arsenic nitride alloys.

4. Conclusions

In conclusion, InGaAlAsPN technology may impact all of the existing III-V technology. Silicon-based epitaxy will enable III-V technology to keep in step with Si technology and wafer size, resulting in a significant reduction in cost of III-V technology. Reliable and high yield monolithic cointegration of lasers, optical detectors, surface acoustic wave filters, microwave circuits and VLSI circuits on a single chip may be possible for the first time, thereby drastically reducing system size and increasing system reliability. To achieve the full potential of this material system further growth studies of the nitride and arsenide nitride materials are needed. The authors would like to acknowledge stimulating discussions with Drs. G. Frazier, T. Moise, J. Randall and A. Seabaugh. The outstanding technical assistance of D. Chasse, A. Fowler, F. Stovall, R. Thomason, and K. Vargason is much appreciated.

References

[1] M. Weyers, M. Sato, H. Ando, Jpn. J. Appl. Phys. **31**, L854 (1992).

[2] M. Weyers and M. Sato, Appl. Phys. Lett. **62**, 1396 (1993).

[3] C. T. Foxon, T. S. Cheng, D. E. Lacklison, S. V. Novikov, D. Johnson, N. Baba-Ali, T. L. Tansley, S. Hooper, and L. J. Challis, 1994 Electronic Mat. Conf. Proc. A35.

[4] S. Bharatan, K. S. Jones, C. R. Abernathy, S. J. Pearton, F. Ren, P. W. Wisk and J. R. Lothian, J. Vac. Sci. and Tech. **A 12**, 1094 (1994).

[5] M. Kondow, K. Uomi, K. Hosomi, T. Mozume, Jpn. J. Appl. Phys. **33**, L1056 (1994).

[6] S. Sakai, Y. Ueta, and Y. Terauchi, Jpn. J. Appl. Phys. **32**, 4413 (1994).

[7] For a review see H. Morkoc, S. Strite, G. B. Gao, M. E. Lin, B. Sverdlov, and M. Burns, J. Appl. Phys. **76**, 1363 (1994).

[8] R. A. Soref, Proc. of the IEEE **81**, 1687 (1993).

[9] G. B. Stringfellow, J. of Cryst. Growth **58**, 194 (1982).

[10] M. J. Jou, Y. T. Cherng, H. R. Jen, G. B. Stringfellow, Appl. Phys. Lett. **52**, 549 (1988).

[11] J. E. Greene, J. of Vac. Sci. and Tech. **B 1**, 229 (1983).

[12] A. A. Mbaye, A. Zunger, D. M. Wood, Appl. Phys. Lett. **49**, 782 (1986).

[13] C. P. Flynn, Phys. Rev. Lett. **57**, 599 (1986).

[14] S.-H. Wei and A. Zunger, Appl. Phys. Lett. **56**, 662, 1990.

[15] D. P. Munich and R. F. Pierret, Solid St. Electron. **30**, 901 (1987).

[16] J. A. Van Vechten and T. K. Bergstresser, Phys. Rev. **B 1**, 3351 (1970).

[17] R. Dornhaus, G. Nimtz, and B. Schlicht, ``Narrow gap semiconductors'', Springer-Verlag, New York (1985).

[18] A. Rubio and M. L. Cohen, Phys. Rev. **B 51**, 4343 (1995).

[19] J. Neugebauer and C. G. Van de Walle, Phys. Rev. **B 51**, 10568 (1995).

[20] S. Tang, T. P. E. Broekaert, and R. M. Wallace, to be published.

[21] J. N. Baillargeon, K. Y. Cheng, G. E. Holfer, P. J. Pearah, K. C. Hsieh, Appl. Phys. Lett. **60**, 2540 (1992).

[22] E. A. Beam III, H.-Y. Liu, and T. P. E. Broekaert, unpublished results.

[23] Y.-C. Kao, W. M. Duncan, H.-Y. Liu, and T. P. E. Broekaert, unpublished results.

Session 3: Posters and Demonstrations (continued)

The Fundamentals of Using the Digital Micromirror Device (DMD™) for Projection Display
by Lars A. Yoder, Texas Instruments

Aercam Demonstration
by Charles Price, NASA/JSC

MEMS Spaceborne Testbed
by Robert H. Stroud, The Aerospace Corporation, and
Mark Holderman, NASA/JSC

Low Volume Packaging for a Microinstrumentation System
by Andrew Mason and Ken Wise, University of Michigan

Pyroelectric Applications of the VDF-TrFE Copolymer
by J.J. Simonne, Laboratoire d'Analyse et d'Architecture des Systèmes,
Ph. Bauer, SOFRADIR, L. Audaire, CEA/DTA/LETI/DOPTS/S-LIR,
and F. Bauer, Institut de Recherche Franco-Allemand de St Louis

Stereo-Based Region-Growing using String Matching
by Robert Mandelbaum and Max Mintz, University of Pennsylvania